Waveguide modulated non-local optical interaction of semiconductor microdisks

Meixin Lei (雷美鑫), Kaijun Che (车凯军)*,

Changlei Guo (郭长磊), Saiyu Luo (罗塞雨), and Zhiping Cai (蔡志平)

School of Information Science and Engineering, Xiamen University, Xiamen 361005, China

**Corresponding author: chekaijun@xmu.edu.cn*

Received January 14, 2014; accepted April 23, 2014; posted online June 26, 2014

The non-local optical interaction of two semiconductor microdisks with a waveguide bridged at radial direction is proposed and studied by three dimensional finite-difference time-domain (FDTD) electromagnetic simulations. The strong and weak optical interactions between two microdisks are observed and ascribed to the internal coupled modes with different coupling ratios. The vertical radiation losses and the related mode quality factors are modulated by waveguide length and present oscillation characteristics for the resonant modes. In addition, the optical leakage of coupling system is affected by the etching depth of disks due to the emission of minor components of electric field.

OCIS codes: 140.4780, 230.4555, 140.3945.

doi: 10.3788/COL201412.071401.

In the past two decades, semiconductor microcavities have attracted considerable attentions for potential applications in microlasers, optical filters, and cavity quantum electro-dynamics[1]. The mostly studied optical mode of microcavity is whispering gallery mode (WGM) with advantages of high quality (Q) factor and small mode volume[2,3]. Recently, photonic molecules, consisting of several circular resonators positioned in a close distance, became a fascinating topic since they can be optimized to exhibit unique optical properties, such as enhancement of mode quality factor, mode splitting and transition etc.[4−16]. Super modes with enhanced Q factor led by decreased radiation loss were observed from coupling of two microdisks[5]. Based on this feature, photonic molecules are regarded as one of the key components for a variety of optical applications, such as low-threshold semiconductor microlasers[14,15], biochemical sensing[6,12], and optical filters[9,13,16]. But for photonic molecules, the common way for photon exchange is via evanescent wave while the attenuating depth of confined optical wave is strongly limited by the high contrast of refractive indices of reflecting interfaces. Therefore, the optical interaction happens only in a short distance and the flexibility of dynamic control on the coupling states is restricted by this feature. To overcome the drawbacks of close coupling, the distant and strong optical coupling is proposed and realized from the two high Q factor photonic crystal (PC) nanocavities which are bridged by a waveguide[17]. A new way for optical processing between two individual photon resonators in a long distance is proposed, even though the needed PC confinement structure is much larger than the nonacavities.

In this letter, a waveguide is bridged between two semiconductor microdisks at radial direction for non-local optical interactions and the confining structure is omitted due to high contrast of refractive indices of materials. The optical system is investigated by three dimensional (3D) finite-differences time-domain (FDTD) electromagnetic simulations, combined with the Padé approximation which is for calculation of resonant spectrum. The results show that the mode Q factors oscillate with the variation of waveguide length, and high Q resonances are observed at conditions of the cancellation of the vertical leakage and the weak optical interaction between two disks. The detailed modes in coupling system are studied by electromagnetic analysis. Moreover, the optimizations of the etching depth of resonator are discussed.

The optical system is comprised of two identical semiconductor microdisks, which are bridged at radial direction by a normal optical waveguide on substrate. The schematic is illustrated in Fig. 1, and the vertical components of disks include an up cladding layer, a center active layer, and a bottom cladding layer with thickness of t_{u}, t_{c}, and t_{b}, respectively. The optical refractive indices of sandwiched disks are set to be 3.17/3.4/3.17, corresponding to InP/InGaAsP/InP semiconductors for laser fabrication. 3D FDTD electromagnetic simulations are performed for investigating the dynamics of optical system[18]. The perfectly matched layers (PMLs) are introduced as absorbing wall for preventing electromagnetic reflection and stopping the electromagnetic computation. The courant time step Δt=0.0577 fs with spatial grids Δx =30 nm, Δy =30 nm, and Δz =30 nm are used. In the simulation, the time variation of magnetic or electric field component at a chosen monitoring

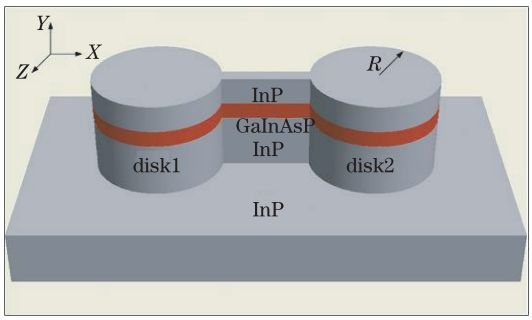

Fig. 1. Schematic illustration of optical interaction system with a waveguide bridged between two semiconductor microdisks at radial direction.

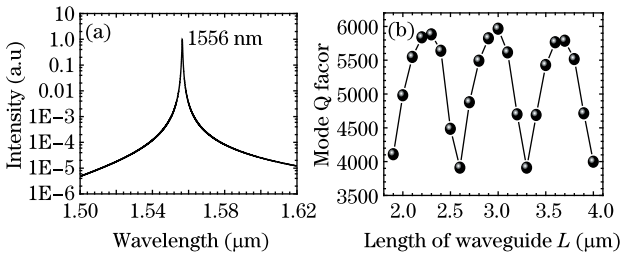

Fig. 2. (a) Typical resonant spectrum of the optical system as R= 2 μm with a 0.3-μm-width waveguide bridged at the radial direction of two disks. (b) The Q factor of resonant mode in the optical system versus the waveguide length L.

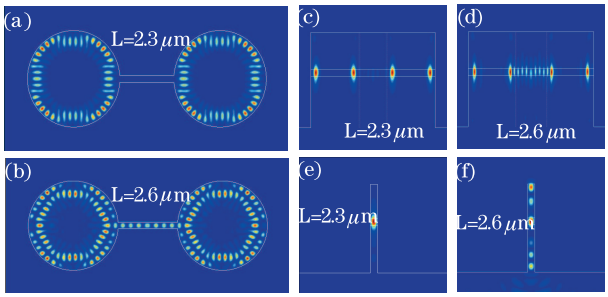

Fig. 3. False-color representations of squared magnetic field $|H_y|^2$ for quasi-TE mode, (a), (c), (e) and (b), (d) ,(f) correspond with L of 2.3 and 2.6 μm respectively.

point inside the resonator is recorded as FDTD output, and the Padé approximation is used to transform the data from the time domain to the frequency domain for obtaining the resonant intensity spectrum[19]. Finally the mode frequencies and Q factors are calculated from the peak frequency and the ratio of the peak frequency to the corresponding 3-dB bandwidth by fitting the peak of the intensity spectra with a Lorentzian function.

Firstly, we studied the influence of waveguide length L on the optical interaction of two disks and only quasi-transverse electric (TE) polarization is considered, since there is no pure TE mode in 3D optical system. Here, the radius of both microdisks is set to be 2 μm, and the width of bridged waveguide is fixed to be 0.3 μm for single mode processing. The vertical structure parameters $t_{\rm u}$, $t_{\rm a}$, and $t_{\rm b}$ are set to be 1.5, 0.3, and 2.1 μm. Figure 2(a) shows a typical resonant spectrum, only one high Q mode is found near optical communication wavelength as the other low Q factor modes are completely decayed. The calculated results indicate that the wavelength of resonant mode near 1556 nm is almost unchanged with the variation of L. As we known, there are two states for the optical resonant system. One is that there is completely no optical interaction between two resonators, the confined optical modes are independent from each other and not affected by the waveguide. The other is that there exists optical coupling between two resonators, and the waveguide only tunes the strength of optical interactions, but due to the self-adaptation of resonant modes in individual resonator (modes with different quantum numbers, but have nearly the same resonant wavelength are coupled with each other)[20], the resonant wavelength thus is slightly tuned by waveguide. The resonant wavelength of both states thus is not affected by L. The Q factors of resonant modes versus L are illustrated in Fig. 2(b), and two important features are found. On one hand, the mode Q factors are tuned by waveguide and present oscillation characteristics. It means that the optical loss or optical interaction of coupling system is periodically influenced by waveguide. On the other hand, the maximum and minimum value keeps nearly constants of 5.8×10^3 and 3.9×10^3, namely, the modes transits between only two states. High and low Q resonances are accompanied weak and strong optical interaction between two microdisks, it also means the scattering loss is great at jointing point of waveguide and microdisks.

In order to intuitively present the resonant mode, in Figs. 3(a) and (b), the false-color representations of squared magnetic field $|H_y|^2$ in the horizontal plane at the active layer are illustrated as L = 2.3 and 2.6 μm respectively. The resonant mode with quadrangle shape in the disks is the dominate mode as L = 2.3 μm. In this resonant mode, the two disks are insulated from each other as the intensity of field in waveguide is very weak, and the mode Q factor keeps constant and is not optically effected by the waveguide. The other state is a high order mode with the mode field fluctuating in radial direction, the optical coupling between disks is obviously observed as the strong field in waveguide is displayed. In this resonant mode, the Q factor of resonant system is productively affected by tuning the waveguide length L. Figures 3(c) and (d) present a slice of false-color representations of $|H_y|^2$ in the cross section of disks, the photons escaped from the disks into waveguide have a great vertical wave vector k_y as L=2.6 μm, the power leakage from the active layer is obviously observed. Figures 3(e) and (f) show the cross section of the waveguide, the vertical power leakage into substrate is further confirmed.

In the following, the detailed modes in coupling system are figured out by electromagnetic analysis. For a two dimensional microdisk with a radius of R and a refractive index of n laterally confined by low refractive index air, the optical field in plane is expressed in polar coordinate:

$$\Phi(r,\,\varphi,\,t)=\sum_{\nu=0}^{+\infty}C_\nu\psi_\nu(r)\mathrm{e}^{\mathrm{i}(\nu\varphi-\omega_\nu t)},\qquad(1)$$

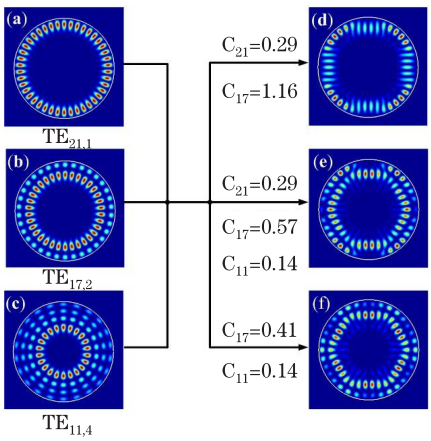

Fig. 4. False-color representations of squared magnetic field $|\mathrm{H}_y|^2$ for (a) $\mathrm{TE}_{21,1}$, (b) $\mathrm{TE}_{17,2}$, and (c) $\mathrm{TE}_{11,4}$ modes. (d) Quadrate-shape coupled mode without optical interaction consisting of $\mathrm{TE}_{21,1}$ and $\mathrm{TE}_{17,2}$ modes. (e) Hexagon-shape coupled mode consists of $\mathrm{TE}_{21,1}$, $\mathrm{TE}_{17,2}$, and $\mathrm{TE}_{11,4}$ modes. (f) Coupled mode with optical interaction consists of $\mathrm{TE}_{17,2}$ and $\mathrm{TE}_{11,4}$ modes.

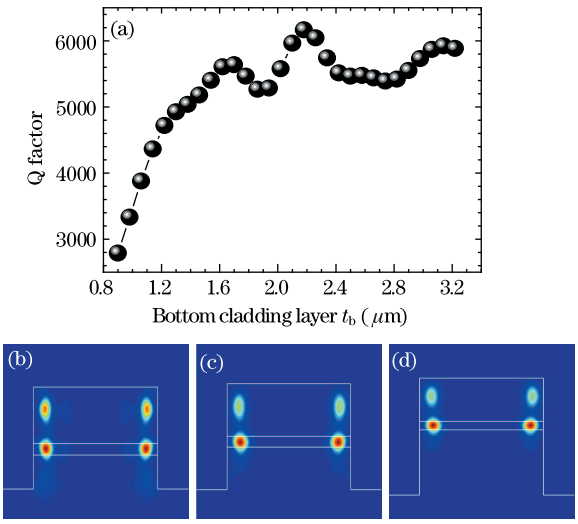

Fig. 5. (a) Mode Q factor versus the etching depth t_b. The false-color representations of electric densities as (b) t_b =0.9, (c) 1.22, (d) 2.26 μm respectively in cross section view of individual disk.

where Φ is the magnetic component H_y or electric component E_y of TE or TM polarization, ν is the azimuthal quantum number, C_ν is the coefficient of corresponding mode, ω_ν is angular frequency, ψ_ν is the field distribution along the radial direction and expressed as

$$\psi_\nu(r) = \begin{cases} J_\nu(nk_0r) & r \leqslant R \\ AH_\nu^{(1)}(k_0r) & r \geqslant R \end{cases}, \quad (2)$$

where k_0 is the wave vector in vacuum, J_ν is the first kind Bessel function, and $H_\nu^{(1)}$ is the first kind Hankle function. Based on the electromagnetic continuity condition at interfaces of different mediums, the mode wavelengths and Q factors of the WGMs can be calculated by

$$J_\nu(nk_0R)H_\nu^{(1)'}(k_0R) = \eta J_\nu'(nk_0R)H_\nu^{(1)}(k_0R) \quad (3)$$

where η is $1/n$ or n for $TE_{\nu,m}$ or $TM_{\nu,m}$, and m denotes radial mode numbers. The eigenvalues are found by transfer matrix method through iterative computation[21]. By using the obtained transverse wave vector or effective index, in Figs. 4(a), (b), and (c), the squared magnetic field $|H_y|^2$ of three typical WGMs ($TE_{21,1}$, $TE_{17,2}$, and $TE_{11,4}$) are presented, the calculated resonant wavelengths are 1548, 1547, and 1546 nm as t_u = 1.5 μm with fixed other structure parameters, which are close to that of numerically obtained 1.556 μm and the error of 0.5% is reasonable due to different techniques of effective index and numerical methods. As we known, when a perfect circular-shaped optical microcavity is broken by a defect (connecting an output waveguide at radial direction for instance), a new resonant mode with weak field near the defect is formed by the self-adjusting of optical field. Namely, the two different WGMs are physically coupled with each other, and the destructive interference happens near the defect for minimizing the emission loss[7,20]. In order to understand the modes in the coupling system, based on the numerically obtained field pattern, we tuned the coefficient C_v. The quadrate-shape coupled mode consisting of $TE_{21,1}$ and $TE_{17,2}$ with coefficients of C_{21}= 0.29 and C_{17}= 0.16 is confirmed while the hexagon-shape mode consists of $TE_{21,1}$, $TE_{17,2}$, and $TE_{11,4}$ modes with C_{21}=0.29, C_{17}=0.57, and C_{11}=0.14. The analytical obtained $|H_y|^2$ are illustrated in Figs. 4(d) and (e), and the patterns are the same as Figs. 3(a) and (b). In order to illustrate the modes which have optical interaction between two disks, by removing redundant optical components without optical interaction, the optical interaction between two disks is only for coupled modes of $TE_{17,2}$ and $TE_{11,4}$ with coefficients C_{17}=0.41 and C_{11}=0.14, Fig. 4(f) shows the modes field pattern.

At last, we consider the effects of the etching depth of microdisk on the dynamics of optical system, the optimization of etching depth can be effectively applied to compress the vertical physical volume of optical system. On one hand, mode Q factor is optimized by the up cladding layer with thickness of t_u = 1.5 μm at which optical waves are firmly confined at active layer and have no leakage to the substrate[22]. The Q factor of coupling system versus t_b is plotted in Fig. 5(a) as L= 3 μm. As expected, once t_b is less than a certain value (1.7 μm), optical waves are emitted into substrate and vertical optical loss of resonant mode becomes greater, the Q factor productively decreases rapidly. As t_b is greater than 1.7 μm, the optical loss is slightly and periodically influenced by t_b as mode Q presents feature of oscillation. To intuitively display the emission of optical wave, in Figs. 5(b)−(d), the electric field densities are illustrated as t_b locating at 0.9, 1.22, and 2.26 μm respectively, the results only show the cross section view of individual disk. The emission of optical wave from the active layer into substrate is obviously observed as t_b =0.9 μm and the main emission is the minor electric component of E_y as the TE field has the same vertical distribution of magnetic field H_y.

In conclusion, a non-local optical interaction system between two semiconductor disks are proposed and studied by 3D FDTD numerical analysis. The strong optical interactions are found from the internal coupled modes with a certain ratio. The optical loss or related Q factor of resonant system is modulated by the bridged waveguide, since the vertical emission losses are affected by waveguide length and the etching depth of disks. The two states of weak and strong coupling are expected as optical switch signals in optical processing system.

This work was supported by the Fundamental Research Funds for the Central Universities (No. 2011121048), the National Natural Science Foundation of China (No. 61107045), and the Open Project of Integrated Optoelectronic State Key Laboratory (No. 2011KFB001).

References

1. K. J. Vahala, Nature **424,** 839 (2003).
2. G. Gu, L. Chen, H. Fu, K. Che, Z. Cai, and H. Xu, Chin. Opt. Lett. **11,** 101401 (2013).
3. C. Dong, C. Zou, J. Cui, Y. Yang, Z. Han, and G. Guo, Chin. Opt. Lett. **7,** 299 (2009).
4. M. Bayer, T. Gutbrod, J. P. Reithmaier, A. Forchel, T. L. Reinecke, P. A. Knipp, A. A. Dremin, and V. D. Kulakovskii, Phys. Rev. Lett. **81,** 2582 (1998).

5. M. Benyoucef, J. B. Shim, J. Wiersig, and O. G. Schmidt, Opt. Lett. **36,** 1317 (2011).
6. S. V. Boriskina, J. Opt. Soc. Am. B **23,** 1565 (2006).
7. K. Che, M. Lei, G. Gu, Z. Cai, and Y. Huang, Appl. Opt. **52,** 8190 (2013).
8. L. I. Deych, C. Schmidt, A. Chipouline, T. Pertsch, and A. Tünnermann, Phys. Rev. A. **77,** 051801 (2008).
9. J. V. Hryniewicz, P. P. Absil, B. E. Little, R. A. Wilson, and P-T. Ho, IEEE Photon. Technol. Lett. **12,** 320 (2000).
10. Y. Huang, J. Lin, Q. Yao, X. Lv, Y. Yang, J. Xiao, and Y. Du, Chin. Opt. Lett. **10,** 091404 (2012).
11. J. Li, J. Wang, and Y. Huang, Opt. Lett. **32,** 1563 (2007).
12. T. W. Lu and P. T. Lee, Opt. Express **17,** 1518 (2009).
13. A. A. Savchenkov, V. S. Ilchenko, A. B. Matsko, and L. Maleki, IEEE Photon. Technol. Lett. 17, 136 (2005).
14. L. Shang, L. Liu, and L. Xu, Opt. Lett. **33,** 1150 (2008).
15. E. I. Smotrova, A. I. Nosich, T. M. Benson, and P. Sewell, Opt. Lett. **31,** 921 (2006).
16. F. N. Xia, M. Rooks, L. Sekaric, and Y. Vlasov, Opt. Express **15,** 11934 (2007).
17. Y. Sato, Y. Tanaka, J. Upham, Y. Takahashi, T. Asano, and S. Noda, Nat. Photon. **6,** 56 (2011).
18. A. Tavlove and S. C. Hagness, *Computational Electrodynamics*: *the Finite-difference Time-domain Method* (Artech House, Norwood, 1995).
19. W. Guo, W. Li, and Y. Huang, IEEE Microw. Wireless Compon. Lett. **11,** 223 (2001).
20. Y. Yang, S. Wang, and Y. Huang, Opt. Express **17,** 23010 (2009).
21. C. C. Katsidis and D. I. Siapkas, Appl. Opt. **41,** 3978 (2002).
22. X. Lv, Y. Huang, Y. Yang, H. Long, L. Zou, Q. Yao, X. Jin, J. Xiao, and Y. Du, Opt. Express **21,** 16069 (2013).